Metrology for Lab-on-a-Chip Final-Product Devices

Darwin R. Reyes,[*] *Michael Halter*[**] *and Jeeseong Hwang*[*]

[*] Physical Measurement Laboratory and [**]Material Measurement Laboratory, National Institute of Standards and Technology, 100 Bureau Drive, Gaithersburg, MD, USA, darwin.reyes@nist.gov

ABSTRACT

New metrology tools to measure the critical parameters of internal structures in Lab-on-a-chip devices are greatly needed in order to develop standard tests for this technology. There is no established method for dimensional measurements of Lab-on-a-chip final- product devices. Here we present a method that combines a custom made optical coherence tomography (OCT) system with an in-house written ImageJ macro to analyze internal structures of poly(methyl methacrylate) (PMMA) Lab-on-a-chip devices. Dimensional information was obtained from OCT images and compared with images acquired using confocal fluorescence microscopy. The results from OCT were validated by those obtained by a well-established technique of confocal imaging of fluorescent fluid confined within the device's channel. This study demonstrates the potential use of the OCT technique in assessing structural information of the sub-surface channels in final-product devices, beyond the reach of confocal microscopy.

Keywords: dimensional metrology, microfluidics, optical coherence tomography, confocal fluorescence microscopy, poly(methyl methacrylate) (PMMA)

1 INTRODUCTION

Researchers in the microfluidics or Lab-on-a-Chip field have been increasingly interested in the standardization of a number of parameters within these devices [1-2], including the internal dimensions of microchannels. The standardization of a non-invasive method capable of measuring the internal dimensions of microchannels in final-products has been of increasing interest in this field. However, finding a method or technique that will be capable of such measurements for a broad range of applications on devices made of different materials will not be trivial.

Robust and validated approaches are required for the measurement of final-product (post assembly) Lab-on-a-chip devices. Techniques used traditionally in the analysis of microelectronic devices that might be also applicable to Lab-on-a-chip devices include scanning probe microscopy (e.g. atomic force microscopy), and optical techniques such as confocal microscopy, ellipsometry and interferometric microscopy. Although these techniques could be used for Lab-on-a-chip devices there are limitations associated to each of them. Scanning probe microscopy provides high resolution dimensional information but the surface needs to be exposed for surface-scanning, the field of measurements is too small, and the probe cannot access to corners of channels in the device. Confocal and interferometric microscopes images within certain distance from the surface as the working distance of these techniques is short, and optical aberration and scattering through the device surface require complex modeling for quantitative interpretation of the measured sub-surface dimensions. OCT is a technique to image deep sub-surface structures through a medium or a set of layered materials, enabling quantitative metrology for final-product Lab-on-a-chip devices.

OCT, an innovative technology most commonly used to image sub-surface structures *in vivo* [3], is based on an optical interferometry principle. Spectral domain OCT uses a broadband near-infrared (NIR) source to generate a set of cross-sectional images in the x- and z-axes (B-scan) by detecting the interface along the z axis (depth, A-scan) from the backscattered light collected at each x coordinate of the specimen (Figure 1, left panel). A tomogram is created when a set of B-scans is generated along the y-axis and is assembled into a volumetric image (Figure 1, center and right panels). Since this technology uses a NIR source, scattering is less significant than in other optical imaging techniques using ultraviolet or visible wavelength light. OCT has the advantages for volumetric imaging, when compared to confocal microscopy, due to a larger depth of imaging (up to around 2 mm) and fast scans of few tens of kilohertz for A-scans.

2 METHODS

2.1 Lab-on-a-chip Devices

PMMA Lab-on-a-chip devices were obtained from a commercial supplier. The dimensions provided by the devices manufacturer are summarized in Table 1.

Table 1. Dimensions of the PMMA devices measured.

DEVICE	WIDTH (µm)	HEIGHT (µm)
A	50	50
B	100	100
C	200	200
D	800	20
E	1000	200

2.2 OCT Imaging

The PMMA devices were imaged using a spectral domain OCT (SDOCT) system operated at a center wavelength of 840 nm with the full-width at half-maximum (FWHM) of 93 nm, producing an FWHM coherence length of about 3 μm. A-scans were collected by a 12 mm focal length telecentric lens over different x-y rectangular areas to form volumetric images into the surface defined by the x-y dimension. The A-scans obtained were analyzed using an ImageJ macro algorithm developed in-house.

2.3 Confocal Microscopy Imaging

Confocal fluorescence images were obtained with a laser-scanning confocal microscope from xz cross-section scans perpendicular to the long direction of the same PMMA microchannels. Lateral and axial resolutions were estimated to be 275 nm and 1.4 μm, respectively.

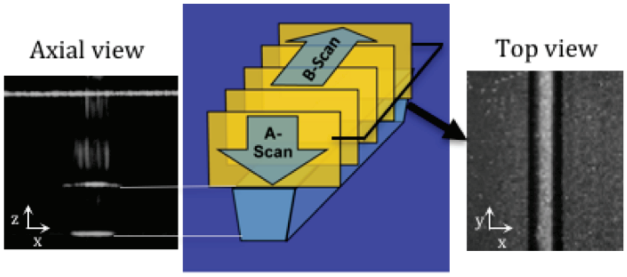

Figure 1. Diagram illustrating the scans (A- and B-scans) executed during the acquiring of optical coherence tomographs. The diagram shows an A-scan of a channel in a Lab-on-a-chip device (left panel). The middle panel shows how the channel is scanned axially and laterally to obtain A-scans and B-scans, respectively. The right panel shows a top view of a collection of B-scans from the same device depicted on the left panel.

2.4 Algorithm used to obtain the dimension of microchannels using OCT

Dimensional information from the OCT images was obtained by using the ImageJ "Default" auto threshold algorithm. Raw OCT images show 2 bright lines from the upper and lower surfaces of the cross-section of the channel defined by the bottom of the channel lid and the bottom of the channel, respectively. The algorithm sequesters pixel locations with intensity higher than the background noise to define the top and bottom boundaries of the channel cross-section (see Fig. 1). After the image was thresholded, along each vertical line in the image, the vertical distance between "the center of mass" intensities was calculated to obtain the depth of the channel. The average width of the channels was determined by obtaining, separately, the width of the upper and lower thresholded surfaces from the bounding box around each surface.

2.5 Algorithm used to obtain the dimension of microchannels using confocal fluorescence microscopy

Dimensional information from the confocal fluorescence images was obtained by first processing the image using the "Default" threshold. This first step was followed by the production of a binary mask image from the applied autothreshold and subsequent one hole filling operation and one erosion step, thus removing stray pixels, at the edge of the image/channel that were above the threshold. The microchannel dimensions (height and upper and lower width) were finally obtained from the processed mask image.

3 RESULTS AND DISCUSSION

3.1 OCT Imaging

OCT images of PMMA Lab-on-a-chip devices, as shown in Fig. 2, were acquired with the OCT system configuration operating in the SDOCT. The internal microchannel structures (top and bottom walls of the channel), which are embedded in the sealed device, are observed in the reconstruction 3D image shown in Fig. 2A. The image illustrates the flat surface of the top and bottom sides of the channels from where the height and width can be obtained. Fig. 2B shows the cross-section (averaged) of all the A-scans depicted in Fig. 2A. Note that the vertical sidewalls of the channel are not resolved due to their steep angles. However, for dimensional measurements of the channels we do not necessarily need the sidewall locations. For example, if a silicon wafer was used as the mold for the PMMA devices, as could be the case for the devices examined here, the average length of the top and bottom surfaces should provide us with the information needed to accurately estimate the area of the channels. This assumption was tested when we compared the OCT measurements with the confocal fluorescence measurements, where all four edges of the channel are determined.

Ninety six (96) xz confocal fluorescence images, for the device that is 50 μm high and 50 μm wide, were processed using an in-house written ImageJ macro. Images were taken in the same region using OCT and processed with the ImageJ macro written for the OCT images (96 images) to determine the height and the average width. The average width refers to the average obtained by first calculating the average width in each image (average of the top and bottom line widths). Then, the overall average width was obtained by taking all the images average widths and calculating the overall average width from them.

Histograms showing the results for the heights and widths measured with OCT and confocal fluorescence demonstrate the overlap that was observed between the repeated measurements (Fig. 3). Figure 3A shows a histogram for the heights measured with confocal fluorescence and OCT. The average value obtained for the measured height with confocal fluorescence was 41 µm ± 1 µm, whereas the average height value with OCT was 48 µm ± 1 µm. The average width values were calculated and plotted in the histogram shown in Fig. 3B. The average widths for both techniques were calculated using the channels top and bottom widths that were measured for the above-mentioned device. In this case the histograms completely overlap showing better agreement between both techniques for the lateral measurements. The average width of the channels measured with confocal fluorescence was 57 µm ± 1 µm, whereas the calculated width obtained with OCT was 56 µm ± 3 µm. We believe that the algorithm developed for the confocal fluorescence images height measurements could be underestimating the height obtained with this technique [4], thus the difference observed between the two set of values.

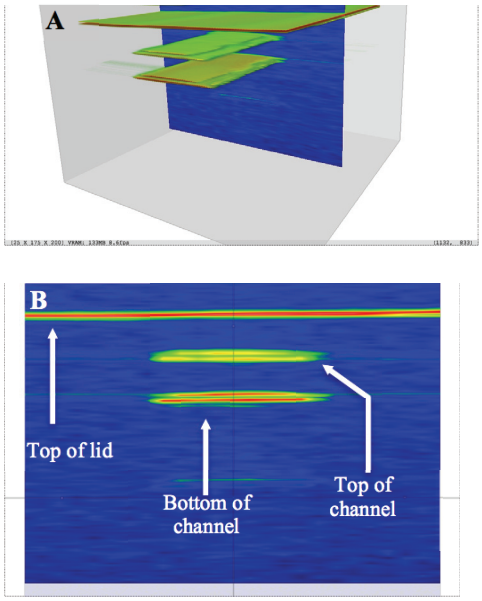

Figure 2. Reconstruction of an OCT B-scan. A) The image shows a 3-dimensional reconstruction of a PMMA channel imaged with OCT. B) Axial representation of all A-scans averaged in the x- and z-axis. The arrows point to the internal structures of the device as well as to the top surface of the lid. The top and bottom sections of the channel can be observed as the average of all the A-scans.

For the two dimensional properties assessed, height and width, the average values obtained with OCT and confocal fluorescence microscopy showed a coefficient of variation (defined as the standard deviation divided by the mean) of 2% and 2.4% for the height, whereas the coefficient of variation for the average width was 1.8% and 5.4% (OCT and confocal fluorescence, respectively).

The data obtained for the heights and widths for all the devices examined was analyzed by comparison with the dimensions reported by the manufacturer (Fig. 4). Plots of dimensions determined by OCT versus the expected dimensions reported by the manufacturer are shown for the measured height (A), average width (B) and area (C), respectively.

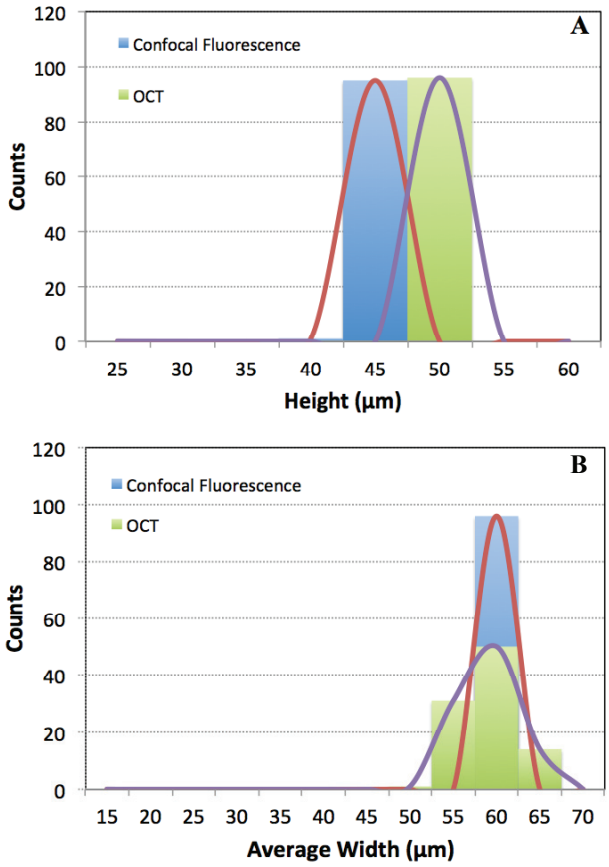

Figure 3. Histograms for the measured height (A) and width (B) with confocal fluorescence microscopy (blue) and OCT (green).

The coefficient of determination, r^2, obtained for the two lines plotted in Fig. 4A were both 0.99 indicating that the regression accounted for a large proportion of the total variability in the observed measured values. Fig. 4B shows the least square regression line for the average width, which generated a coefficient of determination slightly lower, 0.98, but still large enough to assume that for the most part (98%) the total variation in the measured width is explained by the regression. Fig. 4C illustrates the least square regression line for the area computed by OCT versus the expected area based on the manufacturer's reported

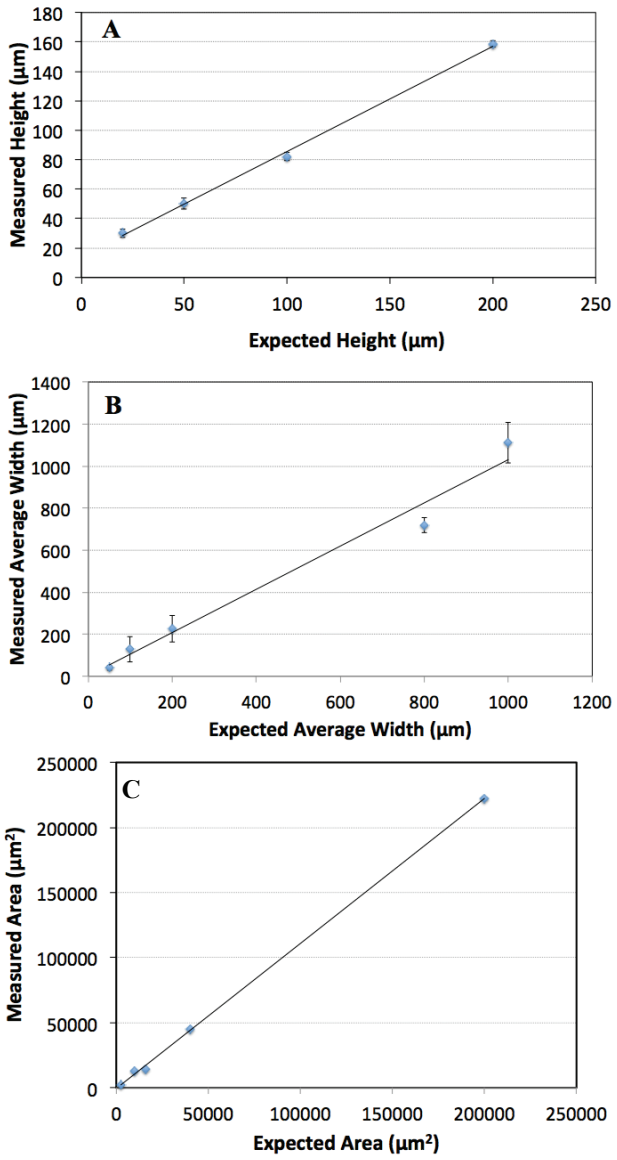

Figure 4. Plots of the measured height (µm), width (µm) and area (µm^2) of the microchannels for the different devices imaged to determine the linear regression on each of the parameters. A) Plot of the measured height of the different channels versus the expected height for each of the structures (based on the height stated by the manufacturer). Notice the two lines from the linear regression fitting are the result of having two devices with the same expected height of 200 µm. The first three points in both plots are the same. B) Plot of the measured average width of the top and bottom widths values obtained from the images. The expected width was chosen based on a square shape microchannels with the top and bottom sides of the channels of the same dimension as the stated by the manufacturer. C) Plot of the measured area of the cross-sections (A-scans) used to calculated the width and height of each channel in the devices tested.

dimensions. For all dimensions, the regression analysis indicates that the OCT measurements accurately predict the actual dimensions reported by the manufacturer.

CONCLUSIONS

We demonstrated for the first time that OCT can be used to image internal structures of polymeric materials, specifically PMMA, and that the measured dimensions are comparable with other well-known confocal fluorescence microscopy technique. The combination of OCT with Image J could allow in the near future for the development of standard tests for the measurement of Lab-on-a-chip final-products internal dimensions. This first demonstration of the use of OCT for dimensional metrology purposes suggests a promising future for this application.

REFERENCES

[1] H. Becker, *Lab on a Chip*, 2010, **10**, 1894.
[2] S. Stavis, *Lab on a Chip*, 2012, **12**, 3008.
[3] B. J. Vakoc, et. al., *Nature Reviews Cancer*, 2012, **12**, 363.
[4] S. Li, et al., *Optics Express*, 2008, **16**, 4001.